ASEAN Engineering Journal

Full Paper

POTENTIAL OF SILVER NANOPARTICLE AS METALLIC BASED PHOTOTHERMAL MEMBRANE FOR SEAWATER DESALINATION USING MEMBRANE DISTILLATION

Parvin a/p Asogan[a], Mohd Hafiz Dzarfan Othman[a]*, Roziana Kamaludin[a], Siti Maryam Jasman[a], Mohd Hafiz Puteh[b], Liew Chia Ming[b]

[a]Advanced Membrane Technology Research Centre (AMTEC), Faculty of Chemical and Energy Engineering, Universiti Teknologi Malaysia, 81310, UTM Johor Bahru, Johor, Malaysia
[b]Department of Environmental Engineering, Faculty of Civil Engineering, Universiti Teknologi Malaysia, 81310, UTM Johor Bahru, Johor, Malaysia

Article history
Received
17 April 2024
Received in revised form
29 August 2024
Accepted
18 September 2025
Published online
30 November 2025

*Corresponding author
hafiz@petroleum.utm.my

Graphical abstract

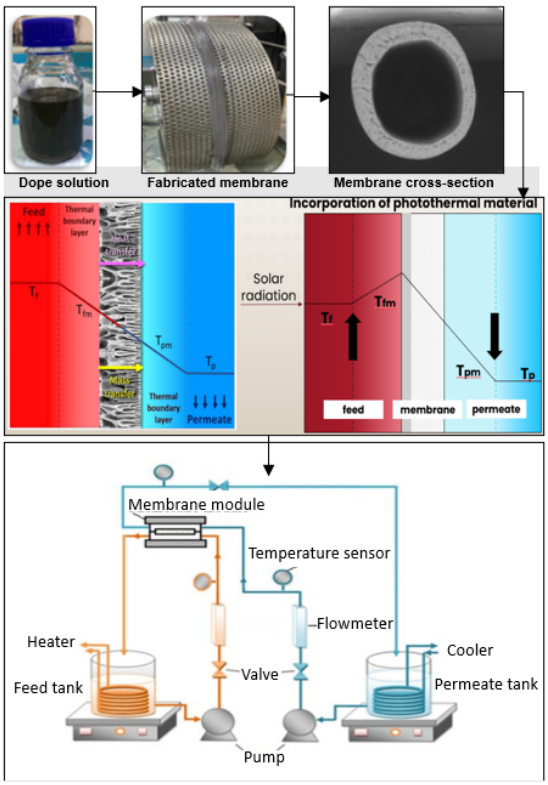

Abstract

Membrane distillation (MD) has emerged as a promising technology for waste purification, driven by its low-energy consumption and high rejection rates. The main challenges encountered in the membrane distillation system revolve around the absence of high-performance membranes and the significant energy demand for heating the feed. In this study, we explore the incorporation of silver nanoparticles into the membrane matrix to enhance the photothermal performance during MD performance. Hollow fiber photothermal membrane was fabricated using non-solvent induced phase separation method (NIPS) by varying the loading of silver nanoparticle to 1 weight percent (wt.%), 1.5wt.% and 2wt.%. A comprehensive analysis of the membrane's photothermal properties, permeability, and selectivity was conducted through various techniques, including scanning electron microscopy (SEM), energy dispersive x-ray (EDX), water contact angle (WCA), liquid entry pressure (LEP), and Ultraviolet-Visible-Near Infrared (UV-Vis NIR). Additionally, the photothermal effectiveness on the membrane distillation performance was evaluated by comparing the water flux and rejection rate of hollow fiber membrane with different silver concentration. The results demonstrate that the integration of silver nanoparticles affects the photothermal efficiency of the membrane leading to better water vapor flux and superior pollutant rejection rates compared to conventional MD membranes. Membrane with concentration of 1.5wt% shows better results with highest contact angle 113.97^{o}, highest LEP of 4.5 bar and permeate flux of 36.47 kg/m^{2}h. The potential benefits of this photothermal membrane for wastewater treatment offers a sustainable and energy-efficient approach to seawater purification, leveraging solar energy to drive the separation process effectively.

Keywords: Membrane distillation, Plasmonic metallic nanoparticle, Hollow fiber membrane, Photothermal effects, Seawater desalination

© 2025 Penerbit UTM Press. All rights reserved

1.0 INTRODUCTION

The present era is grappling with a significant issue of scarcity in having clean freshwater. Several factors such as rising population, enhanced quality of life, a thriving agricultural sector and increased industrialization have exacerbated this problem. It is estimated that over a billion individuals worldwide lack access to uncontaminated freshwater [1]. Traditional energy sources and freshwater reserves are diminishing rapidly. As a result, there is a pressing requirement to create water purification methods that are both less energy-intensive and environmentally friendly. While the total volume of freshwater reservoirs may be sufficient to meet current demands, unfortunately, their distribution does not align with the global population distribution. Approximately 97% of the world's water reserves

are found in the oceans, with only around 3% available as freshwater. The majority of this freshwater is in the form of glaciers and ice caps about 2.06%, with a smaller portion as groundwater approximately 0.90% and other surface freshwater resources about 0.03% [2]. To address the issue of water scarcity, seawater desalination has increasingly become a prominent and widely adopted method for generating accessible water. Nonetheless, most of the current desalination methods including electrodialysis, thermal distillation, and reverse osmosis often involve intricate centralized equipment systems and demand high operating pressures or substantial electrical energy expenses. This undoubtedly poses an economic challenge, particularly for developing nations [3].

Over the past decade, membrane distillation (MD) has gained growing interest as a desalination method, primarily because of several advantages it offers. These benefits encompass operating under lower temperatures in contrast to conventional thermal techniques, facilitation of integration with low-quality energy reservoirs, markedly diminished operational pressure compared to reverse osmosis, decreased susceptibility to membrane fouling, exceptionally elevated efficiency in salt removal and sustained desalination efficacy independent of the salinity level of the feedwater [4]. In desalination processes, MD has the capacity to generate highly pure desalinated water because, in theory, it effectively retains non-volatile substances such as ions, colloids, and large molecules using the membrane. At present, the primary limitation of membrane distillation arises from a phenomenon known as temperature polarization. However, MD is not constrained by polarization phenomena, making it possible to attain recovery rates exceeding 85% [5]. This matter is fundamentally connected to the retrieval of latent heat during water evaporation, causing a gradual decrease in the temperature difference close to the membrane's surface. As a result, the temperature at the interface of the membrane is lower than the temperature of the entire bulk, leading to a decline in the effective force propelling mass transfer. The integration of photothermal materials into the membrane involves the absorption of solar energy to create heat at the interface between the membrane and the feed liquid. This heat is used to facilitate the MD process, offering the benefits of conventional MD while reducing both temperature polarization and energy consumption [3].

Photothermal materials can be broadly categorized into four groups (i) plasmonic particles, (ii) inorganic semiconductor materials, (iii) polymer materials, and (iv) carbon-based materials [6]. By employing photothermal materials, light energy can be transformed into heat at the surface of the membrane. An exemplary illustration of this concept is observed with noble metal nanoparticles. In the case of noble metal nanoparticles, the activation of nanoscale thermal hotspots triggers resonant plasmonic excitations when exposed to light, resulting in localized heating referred to as photothermal excitation [7]. Extensive research is being conducted on noble metals as photothermal conversion materials due to their remarkable thermo plasmonic effect that is initiated by photothermal excitation [8].

Directly integrating metals like silver (Ag) [9] into the process can effectively mitigate temperature polarization in MD thanks to their localized heating properties. However, there was limited research on the utilization of noble metals in MD during the early stages, mainly due to their high cost. In another study, Li et al. [10] directed their attention toward silver nanoparticles, Ag NPs rather than gold nanoparticles, Au NPs. Ag NPs were chosen for their remarkable attributes, which include improved catalytic efficiency, electrical conductivity, chemical durability and light-reflecting properties. The near-field enhancement of Ag NPs was estimated to surpass that of Au NPs by over tenfold, making them particularly advantageous for surface plasmon applications. Additionally, the lower cost of silver makes it a more suitable choice for large-scale technological applications. However, when noble metals are employed, binders are typically used to integrate them into the matrix of polymeric membranes. The initial utilization of noble metals in photothermal membrane distillation (PMD) was documented by Politano et al. [9], who incorporated Ag nanoparticles into PVDF membranes. This was accomplished by directly introducing the nanoparticles into a Dimethylformamide (DMF) solution during the non-solvent-induced phase separation (NIPS) process for vacuum membrane distillation (VMD), which was performed under ultraviolet (UV) light exposure. As a result of incorporating Ag nanoparticles, the membrane exhibited a nine-fold increase in water flux when using 0.5 M sodium chloride (NaCl) as the feed solution. It was confirmed that the inclusion of Ag led to an increase in the temperature polarization factor (TPF), indicating a reduction in temperature polarization [9,11].

In this study, a method for seawater desalination was carried out using metallic based hollow fiber membrane. Silver nanoparticles was incorporated into the fabrication of hollow fiber Polyvinylidene fluoride-silver (PVDF-Ag) nanocomposite membrane. The fabricated membranes were characterized to assess properties such as morphology, hydrophobicity, element composition, wetting resistance and further subjected to membrane performance evaluation. By incorporating silver nanoparticle, we aim to evaluate the potential use of photothermal membrane performance for seawater desalination using membrane distillation.

2.0 METHODOLOGY

2.1 Materials and Reagents

Polyvinylidene fluoride particles bearing the trade designation Kynar 740 (with a molecular weight of 440,000 grams per mole (g/mol)) were procured from Arkema Inc., China. Silver nano powder (AgNP, purity >99.5%, particle size <100 nanometer (nm)) served as the photothermal material. Dimethylacetamide (DMAc, purity >99%, molecular weight = 87.12 g/mol) was utilized as the solvent, sourced from Sigma-Aldrich, while polyethylene glycol (PEG, molecular weight = 3000 g/mol) was incorporated as a pore-forming additive. Sodium hydroxide pellets (NaOH, purity more than 98%, molecular weight = 40 g/mol) were employed for hydroxylation process to bind 1H,1H,2H,2H-Perfluorodecyltriethoxysilane (17-FAS, purity 97%, molecular weight = 610.38 g/mol) on membrane surface, and ethanol with purity >99.9%, molecular weight = 46.07 g/mol was utilized during the membrane fluorination process; both were obtained from Sigma-Aldrich. Sodium chloride (NaCl, purity >99%, molecular weight = 58.44 g/mol) and humic acid (HA), also sourced from Sigma-Aldrich, were utilized to simulate an artificial water source. All substance were used in its original state without additional refinement.

2.2 Dope Formulation and Membrane Fabrication

Prior to dope preparation, PVDF was subjected to drying in a vacuum oven at 60^{o}C for twenty-four hours to eliminate dampness. Before membrane fabrication, 4 sets of dope solutions were prepared: a dope solution without AgNP (denoted as Ag-0), dope solutions with 1wt%, 1.5wt% and 2wt% of AgNP (denoted as Ag-1, Ag-2 and Ag-3 respectively). The chemical compositions of the solution mixtures are detailed in Table 1. Silver nanoparticles (AgNP) and DMAc were combined in a Scott bottle equipped with an overhead stirrer at predetermined quantities. Once the mixture attained homogeneity, the designated amounts of polymer were introduced into the solution. Subsequently, the dope solution was allowed to equilibrate to room temperature and undergo sonication to remove trapped air for 30 minutes prior to fabrication.

Table 1 Compositions of dope solutions

Types of membrane	Dope Composition			
	PVDF	PEG	AgNP	DMAc
Ag-0	18wt%	3wt%	-	79wt%
Ag-1	18wt%	-	1wt%	81wt%
Ag-2	18wt%	-	1.5wt%	80.5wt%
Ag-3	18wt%	-	2wt%	80wt%

Hollow fiber membranes were then produced using the NIPS technique, employing a spinning machine, which aligns with the method previously detailed by our research team [12]. The dope solution was placed into a reservoir, with distilled water being filled in the bore fluid tank. The application of nitrogen pressure facilitated the expulsion of the doping solution from the reservoir. The solution was ejected into a coagulation tank filled with tap water through a spinneret, resulting in membrane formation, which was then collected onto a drum. The precise spinning parameters utilized are outlined in Table 2. Afterward, the accumulated membranes underwent a 24-hour immersion in water to facilitate the diffusion of any residual solvent from within the membranes into the surrounding water. Subsequent to immersion, the hollow fibers were allowed to undergo natural drying.

Table 2 Spinning parameters

Parameter	Specification
Dope flowrate (rpm)	26
Bore fluid flow rate (ml/min)	4
Bore fluid	Distilled water
Coagulant	Tap water
Air gap(cm)	10
Collecting drum speed (rpm)	2~4
Temperature	Room temperature

2.3 Characterization

2.3.1 Scanning Electron Microscopy (SEM)

High-definition images of membrane morphological structures for all samples, both pre- and post-coating, were analyzed via SEM (TM 3000, Hitachi). To analyze the surface morphology, the membrane was placed horizontally on a rectangular plate. To analyze the cross-section, the membrane was broken using nitrogen liquid and then allocated vertically on the plate. To secure the membranes onto the plate, carbon conductive tapes were used. Prior to the process, platinum was used to coat the membrane and the analysis was carried out in a vacuum environment. The SEM images were captured at various scale for observation to provide a comprehensive examination of the membrane structure and morphology.

2.3.2 Electron Dispersive X-ray (EDX)

With regards to the used nanoparticles, the distributed elements within the membranes were assessed through the EDX analysis employing a variable pressure scanning electron microscope with model JEOL JSM-IT300LV. The membrane was placed horizontally on a rectangular stud with carbon conductive tape. The images were captured for observation to provide a comprehensive examination of the existing elements.

2.3.3 Water Contact Angle (WCA)

A goniometer (Model G1, Kruss GmbH, Hamburg, Germany) was used to measure the water contact angle of the membranes. To ascertain the contact angle of the outer layer, a 0.5 µL drop of water was administered onto the exterior of the membrane via a vertically clamped syringe, employing the sessile drop technique. Subsequently, the membrane surface underwent meticulous scrutiny, and the contact angle was quantified utilizing a high-resolution camera. The measurement of the contact angle was conducted at multiple area on the membrane, with the resultant mean outcome value computed. The process of determining the sliding angle involves placing a minuscule droplet of deionized water, which is 1µm in size, on the surface of the membrane. Then, the stage was manually tilted to allow the droplet to slide off the surface. Throughout the procedure, a high-resolution camera was used to document the process.

2.3.4 Liquid Entry Pressure (LEP)

In evaluating the membrane's resistance to wetting, LEP assessment was performed. The membrane, housed within an adapter, underwent testing within a module wherein one part surface of the membrane's lumen was enclosed with resin glue. Compressed nitrogen was utilized to drive water into the membrane. Incremental pressure of 0.5 bar were applied every 5 minutes until the membrane exhibited its initial water droplet leakage. This testing protocol was repeated a minimum of three times to ascertain the mean value.

2.3.5 Ultraviolet-Visible-Near Infrared (UV-Vis NIR)

UV-vis NIR was used to investigate the photothermal effect of a material by monitoring changes in its optical properties when it absorbs light. During the test, the sample is exposed to UV or visible light, and the absorption of the light is measured as a function of time. When the sample absorbs light, it can undergo photothermal heating causing changes in its temperature, and subsequently, changing its optical properties. These changes were detected by measuring the absorption spectra of the sample before and after exposure to light. UV-vis NIR can show the absorbance of a material and measures the amount of light absorbed by a material as a function of the

wavelength of the light. UV-vis spectra show a plot of absorbance (or sometimes transmittance) on the y-axis versus the wavelength of light on the x-axis.

2.4 Direct Contact Membrane Distillation (DCMD)

Prior to performance evaluation, a membrane module was created for the operation of DCMD for processing the mimic of water source, using a method that closely followed a previously established procedure with minimal adjustments [4,13]. A feed solution with a concentration of 35,000 ppm was prepared by dissolving 140 g of sodium chloride and 0.4 g of humic acid in 4,000 mL of distilled water. The conductivity of the feed solution was assessed using a Thermo Scientific conductivity meter before the experiment. The DCMD configuration was operational for a duration of three hours. The solution that permeated through was measured using a precision weighing balance and the weight was used to determine the permeate flux as well as the conductivity was measured to determine the rejection rate for every 20 minutes throughout the experiment. A comprehensive description of the DCMD setup was referred from earlier work [4,14]. The parameters managed in this experiment are listed in Table 3.

Table 3 Parameters of DCMD

Parameter	Value
Concentration of feed solution (g/L)	35
Feed temperature(^{o}C)	85
Feed flowrate(LPM)	0.1
Permeate temperature(^{o}C)	10
Permeate flowrate(LPM)	0.1

3.0 RESULTS AND DISCUSSION

3.1 Morphology

The morphology for the cross section of the hollow fiber membrane can be seen from SEM images as shown in Figure 1. Depicted in Figure 1, the cross section of outer and inner part has developed finger-like structures. Using varying amounts of additives in the production of membranes may lead to the creation of diverse structures in the resulting hollow fiber membranes [15]. As for Ag-0 membrane, it was expected to exhibit longer finger like structures with the addition of PEG as reported by Galiano et al. [16] who obtained an almost similar structure. Even though with the increase in nanoparticle concentration from Ag-1 to Ag-3, it can be noticed that the SEM analysis reveals a higher amount of concentration on membrane surface of Ag-2 compared to Ag-3. The possibility of this outcome could be due to the non-homogeneity of dope solution and its high viscosity which hinder the dispersion of particles within the solution causing it to not maintain uniform dispersion within the dope [17]. As a result, regions with a higher concentration of particles leads to the formation of agglomerates thus affecting the membrane fabrication process.

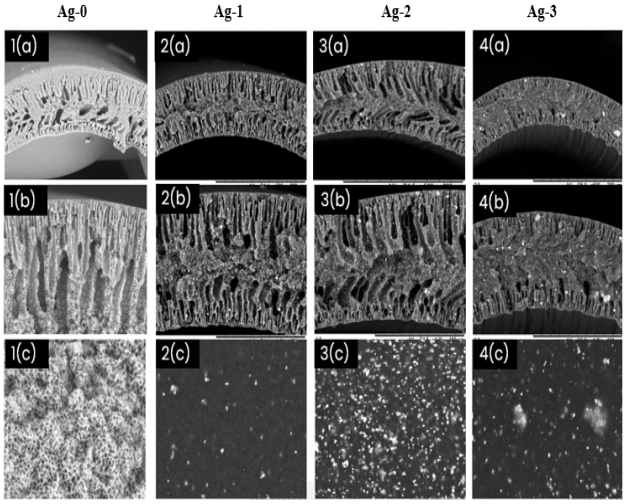

Figure 1 SEM images of Ag-0, Ag-1, Ag-2 and Ag-3 membrane with different magnifications a) 500x b) 1kx c) 2kx

As shown in Table 4 the nanocomposite membranes Ag-1 to Ag-3 exhibits greater thickness compared to pristine membrane, Ag-0. It can be observed that there was no consistency in the outer diameter trend which could be due the inhomogeneity and high viscosity of dope solution along with its uneven distribution of nanoparticle during fabrication for membrane Ag-3. However, the addition of nanoparticle along with the increase in concentration resulted in an elevation of the dope solution's viscosity, consequently causing an augmentation in membrane thickness [18].

Table 4 Thickness of membrane (number of readings, n=3)

Membrane	Outer diameter (mm)	Thickness (mm)
Ag-0	1.36±0.008	0.130±0.005
Ag-1	0.953±0.001	0.226±0.001
Ag-2	1.15±0.01	0.347±0.001
Ag-3	1.06±0.01	0.451±0.001

3.2 Element Composition

The mapping of the atoms and the mass percentage of atoms between the nanocomposite and pure membrane are as illustrated in Figure 2 and 3. Figure 2 depicts that membrane Ag-0 shows no sign of Ag atoms and membrane Ag-2 has the highest distribution of Ag on membrane surface due to better distribution of nanoparticle on surface compared to Ag-3.

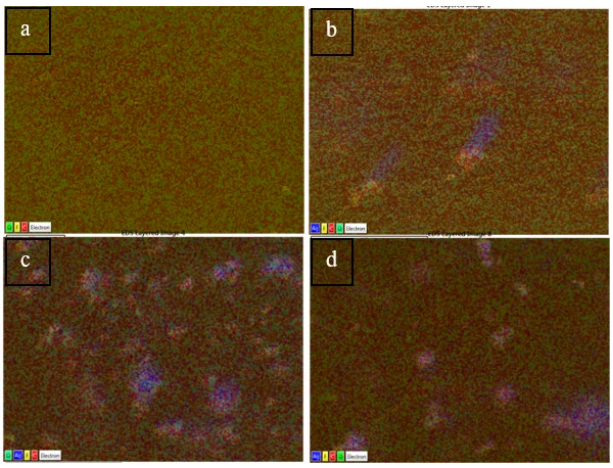

Figure 2 EDX images of membrane with different concentration of nanoparticles a)Ag-0 b)Ag-1 c) Ag-2 d) Ag-3

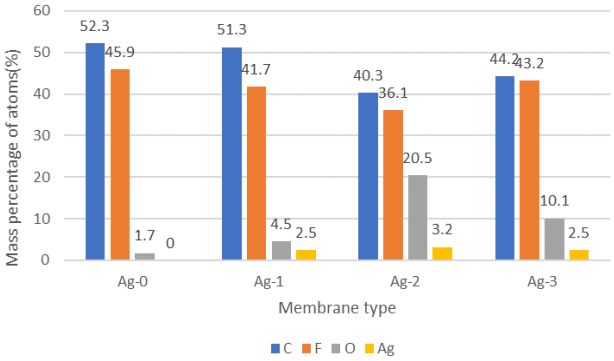

Figure 3 Mass percentage of atoms in membrane

The PVDF polymer contains carbon (C) and fluorine (F) atoms in its main repeating unit -(CH2-CF2)- and along with the addition of DMAc (dimethylacetamide) which is an organic solvent that contains carbon (C), hydrogen (H), oxygen (O), and nitrogen (N) atoms. In addition, the presence of silver (Ag) atoms was through the addition of silver nanoparticles. According to Figure 3, the Ag-0 membrane shows no presence of Ag atoms as no silver particles were added and it was used as a control. However, it can be noticed that the mass percent of Ag is at the highest within membrane Ag-2 with mass percentage of 20.5% and the lowest within membrane Ag-1 with mass percentage 4.5%. Membrane Ag-3 was noted to not achieve the highest Ag mass percentage due to its uneven distribution as the dope was too viscous causing uneven distribution of nanoparticle during fabrication. Fenouillot et al. [17] reported that viscosity significantly influences localization of nanoparticles in polymer blends.

3.3 Water Contact Angle

Silver nanoparticles (AgNPs) have been reported to cause PVDF membranes to become more hydrophilic by reducing their contact angle, which is a measure of surface wettability [19]. Table 5 shows the tabulated data of contact angle for three readings before and after coating along with its percentage error to study membrane hydrophobicity.

Table 5 Contact angle before and after coating (number of samples, n=3)

Membrane	CA before coating (°)	CA after coating (°)
Ag-0	86.34±5.78	124.43±2.61
Ag-1	79.93±3.75	103.43±1.85
Ag-2	76.90±1.59	113.97±2.23
Ag-3	73.48±5.98	107±5.26

Figure 4 shows the trend for contact angle of membrane before and after coating with 1H,1H,2H,2H-perfluorodecyltriethoxysilane (FAS). Prior to coating, the contact angle of membrane decreased from 86.34° to 73.48° with the addition of silver nanoparticle. Subsequent to coating, an elevation in contact angle was recorded. However, the increase was not linear after FAS coating from Ag-1 to Ag-3 due to uneven coating on Ag-3 which was the earlier caused of agglomeration of nanoparticle during the membrane fabrication which have impacted the morphological property of membrane.

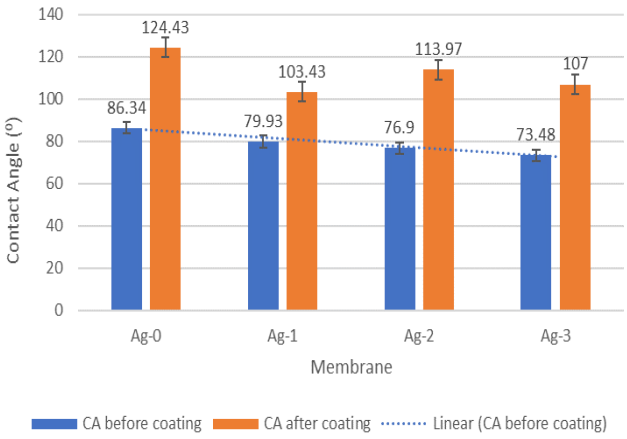

Figure 4 Contact angle of all fabricated membrane before and after coating

3.4 Liquid Entry Pressure (LEP)

The ability of membrane to resist wetting was determined by the measurement of LEP, which referred to the lowest hydrostatic pressure that had to be exert to a liquid, like water in this case, to penetrate and wet the hydrophobic membrane. The LEP value indicates the importance of a good wetting resistance in a membrane and a desired LEP value is usually above 2.5 bar [20]. Membrane that has a constant pore shape and is in contact with a liquid on its surface, an elevated contact angle and reduced pore size result in an increased liquid entry pressure (LEP). Table 6 shows the mean pore size obtained by each of the membrane. The pore sizes of membranes employed in MD application should range from 10 nm to 1 µm. To prevent pore wettability, the membrane material should be hydrophobic, featuring a higher water contact angle and a small maximum pore size [21,22].

Table 6 Pore size of membranes

Membrane	Pore size (µm)	LEP (bar)
Ag-0	0.031±0.027	5
Ag-1	0.107±0.869	3.5
Ag-2	0.103±0.871	4.5
Ag-3	0.144±0.341	0.5

This increase in LEP is attained by enhancing hydrophobicity, which involves reducing the surface energy of the membrane which can be observed from Figure 5 where membrane Ag-0 which has the highest contact angle of 124.43° having the highest LEP value of 5 bars. Membrane Ag-1 to Ag-3 were unable to achieve the similar LEP value as Ag-0 due to the addition of silver nanoparticle into the polymer which are more hydrophilic in nature. Membrane Ag-0, a neat PVDF membrane which has hydrophobic nature and low surface energy contributed to better wetting resistance compared to other membranes where with the addition of silver nanoparticles, the membranes were more prone to wetting. Membrane Ag-3 was noticed to have a drastic drop with LEP value of 0.5 bar compared to Ag-1 and Ag-2 with LEP value of 3.5 bar and 4.5 bar respectively. The decrease in LEP value for membrane Ag-3 could be related to its uneven distribution and agglomeration of nanoparticle during fabrication which may have cause a defect in its morphological property which disallows membrane to withstand high pressure. Younas [23] stated that the mechanical strength of a membrane is largely influenced by its morphology.

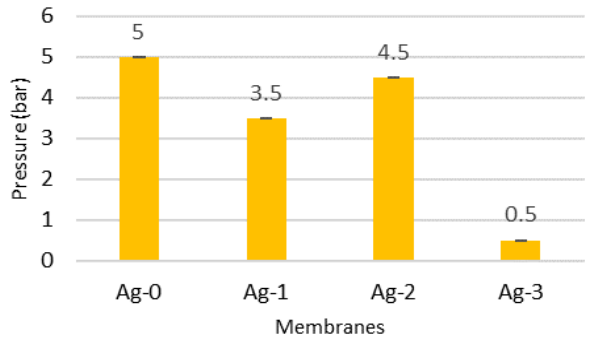

Figure 5 LEP value for all fabricated membrane after FAS coating (number of samples, n=3)

3.5 UV-vis NIR

The optical characteristics of PVDF and PVDF-Ag were confirmed by UV-vis NIR over the range 200–800 nm as depicted in Figure 6. As shown, an absorption edge for membrane Ag-0 was observed at wavelength 254 nm with absorbance of 0.7%, Ag-1 at wavelength 337nm with absorbance of 0.52%, Ag-2 at wavelength 333 nm with absorbance of 0.25 % and Ag-3 at wavelength 331 nm with absorbance of 0.37%. According to a study, a distinct absorption peak in pure PVDF material at a wavelength of 240 nm was detected indicating the semicrystalline nature of PVDF and PVDF incorporated with silver demonstrate a distinct optical response within the wavelength range of 372–424 nm [20]. In another study of silver-polyvinylpyrrolidone (AG-PVP), the composite film showed an absorbance of 0.10~0.125% at wavelength between 300~350 nm [24]. According to Palanisamy [25], as the concentration of gold nanoclusters increases, the absorbance increases as well. However, comparing Ag-1, Ag-2, and Ag-3, it was noticed that membrane Ag-1 with the lowest silver concentration has the highest absorbance value and Ag-2 with lowest absorbance value. There was no clear trend noticed in absorbance value possibly due to the agglomeration and uneven distribution of silver nanoparticle during fabrication of membrane.

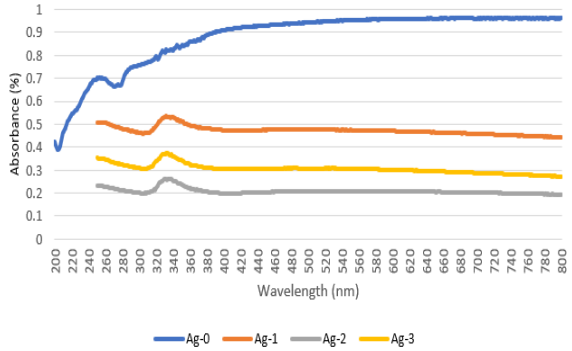

Figure 6 Comparison of absorbance spectra of PVDF-based hollow fiber membrane with addition of silver nanoparticle

3.6 Performance Test

The rate of mass transfer in membrane distillation is directly correlated with the magnitude of the driving force, which is contingent upon the temperature gradient between the distillate streams and feed. The driving force for mass transfer in membrane distillation is the distinction in vapor pressure between the feed and distillate streams, which is related to their temperature difference. As the temperature difference between the two streams increases, the vapor pressure difference also increases, resulting in a higher driving force for mass transfer and thus a higher flux. Figure 7(a) shows the permeate flux acquired for all fabricated membranes. The permeate solution was weighed using a weighing balance and the weight was used to determine the permeate flux as well the conductivity was measured to determine the rejection rate for every 20 minutes for 3 hours duration.

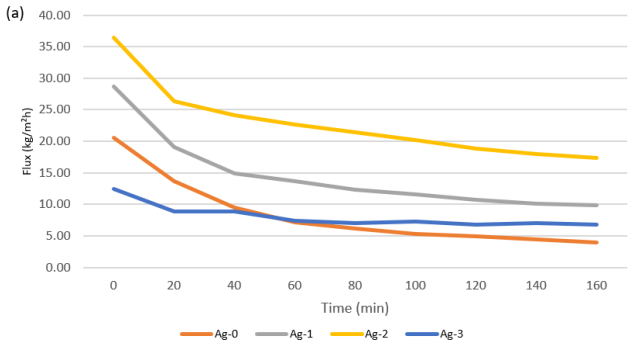

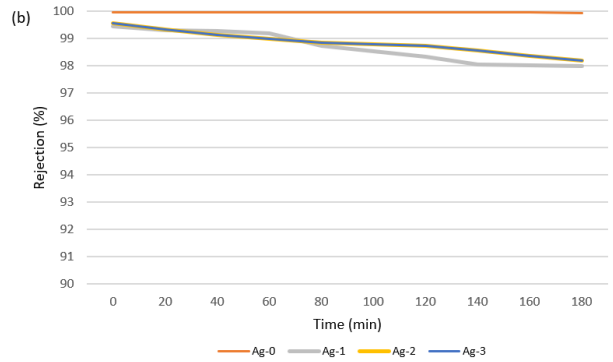

Figure 7 Performance of all fabricated membrane (a) Membrane flux (b) Rejection rate

All the fabricated membranes showed a rejection rate between 98% to 100% with the neat membrane having the highest rejection rate as shown in figure 7(b). The nanocomposite membrane shows to have a higher flux than the neat membrane. The addition of silver nanoparticle has potentially allowed the silver nanoparticles on membrane to undergo plasmon resonance which might have potentially improved the flux. The interaction of incident light with the metal surface causes the free electrons on the surface to oscillate collectively and produces heat which could increase or maintain temperature. However, membrane Ag-2 has higher flux compared to membrane Ag-3 due to the higher mass percent of silver on its surface as shown in the EDX analysis. Even though, membrane Ag-3 was expected to achieve the best result due to its highest Ag concentration, but uneven distribution and agglomeration has deteriorated membrane quality.

4.0 CONCLUSION

Photothermal hollow fiber membranes incorporating silver nanoparticles was successfully fabricated via NIPS technique. The addition of different Ag nanoparticle loading has significantly affected the membrane performance. Notably, membrane Ag-2 with loading of 1.5wt.% gave better results in comparison to membrane Ag-1 and Ag-3. However, it was noted that membrane Ag-0 obtained a higher contact angle of (124.43^{o}±2.61) compared to Ag-2 (113.97^{o}±2.23) which had a slight drop due to presence of silver nanoparticles having its hydrophilic properties but still managed to achieve a hydrophobic surface with coating of 17-FAS. Membrane Ag-2 has an LEP value of 4.5 bar where a 10% difference can be noticed with membrane Ag-0. It can be observed that membrane Ag-2 has a longer finger liked structures and a higher displacement of silver nanoparticle achieving up to 20.5% was measured on the surface. Membrane Ag-2 was able to achieve highest permeate flux of 36.47 kg/m^{2}h with an increment of nearly 77.6 % compared to the neat membrane, 20.53 kg/m^{2}h. Findings in this study highlight the promising potential of silver nanoparticle as a viable solution for photothermal membrane using membrane distillation. In essence, the initial application of seawater desalination sets the stage for the potential advancement of a membrane technology that is both environmentally sustainable and economically feasible.

Acknowledgement

The authors would like to acknowledge the financial support from the Ministry of Higher Education Malaysia under Fundamental Research Grant Scheme (FRGS/1/2023/TK05/UTM/01/2 / R.J130000.7809.5F669) and Universiti Teknologi Malaysia UTM High Impact Research (Q.J130000.2409.08G34) and Fantastic Four (Q.J130000.4622.00Q17). The authors would like to acknowledge the technical and management support from Research Management Centre (RMC), Universiti Teknologi Malaysia.

Credit Author Statement: Parvin Asogan: Writing- Original draft preparation & Editing. **Roziana Kamaludin:** Review & Editing. **Mohd Hafiz Dzarfan:** Supervision, Funding Acquisition. **Mohd Hafiz Puteh:** Validation.

Conflicts of Interest: The writers affirm that they have no financial or other conflicts of interest.

Data Availability: As the data is also a part of an ongoing investigation, the information needed to replicate these results cannot currently be disclosed

Conflicts of Interest

The author(s) declare(s) that there is no conflict of interest regarding the publication of this paper

References

[1] Drioli, E., Ali, A., & Macedonio, F. 2015. Membrane distillation: Recent developments and perspectives. *Desalination*, *356*: 56–84. DOI: https://doi.org/10.1016/j.desal.2014.10.028

[2] Shirazi, M. M. A., Kargari, A., & Shirazi, M. J. A. 2012. Direct contact membrane distillation for seawater desalination. *Desalination and Water Treatment*, *49*(1–3): 368–375. DOI: https://doi.org/10.1080/19443994.2012.719466

[3] Ding, S., Zhang, T., Wu, M., & Wang, X. 2023. Photothermal dual-layer hydrophilic/hydrophobic composite nanofibrous membrane for efficient solar-driven membrane distillation. *Journal of Membrane Science*, *680*: 121740. DOI: https://doi.org/10.1016/j.memsci.2023.121740

[4] Ravi, J., Othman, M. H. D., Tai, Z. S., El-Badawy, T., Matsuura, T., & Kurniawan, T. A. 2021. Comparative DCMD performance of hydrophobic-hydrophilic dual-layer hollow fibre PVDF membranes incorporated with different concentrations of carbon-based nanoparticles. *Separation and Purification Technology*, *274*: 118948. DOI: https://doi.org/10.1016/j.seppur.2021.118948

[5] Wang, P., & Chung, T. 2015. Recent advances in membrane distillation processes: Membrane development, configuration design and application exploring. *Journal of Membrane Science*, *474*: 39–56. DOI: https://doi.org/10.1016/j.memsci.2014.09.016

[6] Razaqpur, A. G., Wang, Y., Liu, X., Liao, Y., & Wang, R. 2021. Progress of photothermal membrane distillation for decentralized desalination: A review. *Water Research*, *201*: 117299. DOI: https://doi.org/10.1016/j.watres.2021.117299

[7] Xu, G., Wang, M., Xu, K., Zhao, H., & Liu, Q. 2023. Membrane fabrication and configuration design development of photothermal membrane distillation (PMD). *Desalination*, *565*: 116833. DOI: https://doi.org/10.1016/j.desal.2023.116833

[8] Gong, C., & Leite, M. S. 2016. Noble metal alloys for plasmonics. *ACS Photonics*, *3*(4): 507–513. DOI: https://doi.org/10.1021/acsphotonics.5b00586

[9] Politano, A., Di Profio, G., Sanna, V., Cupolillo, A., & Curcio, E. 2019. Overcoming temperature polarization in membrane distillation by thermoplasmonic effects activated by Ag nanofillers in polymeric

membranes. *Desalination*, *451*: 192–199. DOI: https://doi.org/10.1016/j.desal.2018.03.006

[10] Li, H., Liu, Z., Jiang, B., & Huang, Y. 2017. A flexible thin-film membrane with broadband Ag@TiO2 nanoparticle for high-efficiency solar evaporation enhancement. *Energy*, *139*, 210–219. DOI: https://doi.org/10.1016/j.energy.2017.07.180

[11] Politano, A., Argurio, P., Di Profio, G., Sanna, V., Cupolillo, A., Chakraborty, S., Arafat, H. A., & Curcio, E. 2016. Photothermal membrane distillation for seawater desalination. *Advanced Materials*, *29*(2). DOI: https://doi.org/10.1002/adma.201603504

[12] Dzinun, H., Othman, M. H. D., Ismail, A. F., Puteh, M. H., & Rahman, M. A. 2015. Photocatalytic degradation of nonylphenol by immobilized TiO2 in dual layer hollow fibre membranes. *Chemical Engineering Journal*, *269*: 255–261. DOI: https://doi.org/10.1016/j.cej.2015.01.114

[13] [13] El-Badawy, T., Othman, M. H. D., Norddin, M., Matsuura, T., Adam, M. R., Ismail, A. F., Tai, Z. S., Zakria, H., Edalat, A., Jaafar, J., Rahman, M. A., Usman, J., Ojo, S., & Malah, M. 2022. Omniphobic braid-reinforced hollow fiber membranes for DCMD of oilfield produced water: The effect of process conditions on membrane performance. *Journal of Water Process Engineering*, *50*: 103323. DOI: https://doi.org/10.1016/j.jwpe.2022.103323

[14] Hubadillah, S. K., Othman, M. H. D., Ismail, A. F., Rahman, M. A., & Jaafar, J. 2019. A low-cost hydrophobic kaolin hollow fiber membrane (h-KHFM) for arsenic removal from aqueous solution via direct contact membrane distillation. *Separation and Purification Technology*, *214*: 31–39. DOI: https://doi.org/10.1016/j.seppur.2018.04.025

[15] [15] Arahman, N., Mulyati, S., & Fahrina, A. 2019. Morphology and performance of pvdf membranes composed of triethylphospate and dimethyl sulfoxide solvents. *Materials Research Express*, *6*(6): 066419. DOI: https://doi.org/10.1088/2053-1591/ab1032

[16] Galiano, F., Xue, S., Marino, T., Boerrigter, M., Saoncella, O., De Simone, S., Faccini, M., Chaumette, C., Drioli, E., & Figoli, A. 2018. Novel Photocatalytic PVDF/Nano-TIO2 hollow fibers for environmental remediation. *Polymers*, *10*(10): 1134. DOI: https://doi.org/10.3390/polym10101134

[17] Fenouillot, F., Cassagnau, P., & Majesté, J. (2009). Uneven distribution of nanoparticles in immiscible fluids: Morphology development in polymer blends. *Polymer*, *50*(6): 1333–1350. DOI: https://doi.org/10.1016/j.polymer.2008.12.029

[18] Abdel-Karim, A., Luque-Alled, J. M., Leaper, S., Alberto, M., Fan, X., Vijayaraghavan, A., Gad-Allah, T. A., El-Kalliny, A. S., Székely, G., Ahmed, S. I., Holmes, S. M., & Gorgojo, P. 2019. PVDF membranes containing reduced graphene oxide: Effect of degree of reduction on membrane distillation performance. *Desalination*, *452*: 196–207. DOI: https://doi.org/10.1016/j.desal.2018.11.014

[19] Alnairat, N., Dalo, M. A., Abu-Zurayk, R., Mallouh, S. A., Odeh, F., & Bawab, A. A. 2021. Green synthesis of silver nanoparticles as an effective antibiofouling material for polyvinylidene fluoride (PVDF) ultrafiltration membrane. *Polymers*, *13*(21): 3683. DOI: https://doi.org/10.3390/polym13213683

[20] Ponelyte, S., & Palevičius, A. 2014. Novel piezoelectric effect and Surface plasmon Resonance-Based elements for MEMS applications. *Sensors*, *14*(4): 6910–6921. DOI: https://doi.org/10.3390/s140406910

[21] Tai, Z. S., Aziz, M. H. A., Othman, M. H. D., Ismail, A. F., Rahman, M. A., & Jaafar, J. 2019. An overview of membrane distillation. In *Elsevier eBooks* 251–281. DOI: https://doi.org/10.1016/b978-0-12-812815-2.00008-9

[22] El-Bourawi, Ding, Z., Ma, R., & Khayet, M. 2006. A framework for better understanding membrane distillation separation process. *Journal of Membrane Science*, *285*(1–2): 4–29. DOI: https://doi.org/10.1016/j.memsci.2006.08.002

[23] Younas, H., Afridi, Z. U. R., Zhou, Y., & Cui, Z. 2020. Progress and perspective of antifouling, pressure driven, Flat-Sheet nanocomposite, polymeric membranes in water treatment. *Journal of Membrane Science and Research*, *6*(3): 319–332. DOI: https://doi.org/10.22079/jmsr.2020.117983.1312

[24] Wang, L., Zhang, T., Zhang, X., Song, Y., Li, R., & Zhu, S. 2014. Optical properties of Ag nanoparticle-polymer composite film based on two-dimensional Au nanoparticle array film. *Nanoscale Research Letters*, *9*(1). DOI: https://doi.org/10.1186/1556-276x-9-155

[25] Palanisamy, S. 2014. Polydopamine supported gold nanoclusters for sensitive and simultaneous detection of dopamine in the presence of excess ascorbic acid and uric acid. *Electrochimica Acta*, *138*: 302–310. DOI: https://doi.org/10.1016/j.electacta.2014.06.13